

# Are both BL Lacs and pulsar wind nebulae the astrophysical counterparts of IceCube neutrino events?

P. Padovani<sup>1</sup> and E. Resconi<sup>2\*</sup>

<sup>1</sup>*European Southern Observatory, Karl-Schwarzschild-Str. 2, D-85748 Garching bei München, Germany*

<sup>2</sup>*Technische Universität München, James-Frank-Str. 1, D-85748 Garching bei München, Germany*

11 June 2014

## ABSTRACT

IceCube has recently reported the discovery of high-energy neutrinos of astrophysical origin, opening up the PeV ( $10^{15}$  eV) sky. Because of their large positional uncertainties, these events have not yet been associated to any astrophysical source. We have found plausible astronomical counterparts in the GeV – TeV bands by looking for sources in the available large area high-energy  $\gamma$ -ray catalogues within the error circles of the IceCube events. We then built the spectral energy distribution of these sources and compared it with the energy and flux of the corresponding neutrino. Likely counterparts include mostly BL Lacs and two Galactic pulsar wind nebulae. On the one hand many objects, including the starburst galaxy NGC 253 and Centaurus A, despite being spatially coincident with neutrino events, are too weak to be reconciled with the neutrino flux. On the other hand, various GeV powerful objects cannot be assessed as possible counterparts due to their lack of TeV data. The definitive association between high-energy astrophysical neutrinos and our candidates will be significantly helped by new TeV observations but will be confirmed or disproved only by further IceCube data. Either way, this will have momentous implications for blazar jets, high-energy astrophysics, and cosmic-ray and neutrino astronomy.

**Key words:** BL Lacertae objects: general — gamma-rays: galaxies — neutrinos — pulsars: general — radiation mechanisms: non-thermal

## 1 INTRODUCTION

The IceCube South Pole Neutrino Observatory<sup>1</sup> has reported the first evidence of high-energy astrophysical neutrinos<sup>2</sup> (Aartsen et al. 2013; IceCube Collaboration 2013), and more recently has confirmed and strengthened these observations by publishing a sample of 35 events with a deposited energy from 30 TeV to 2 PeV (IceCube Collaboration 2014). With this enlarged sample the null hypothesis that all events are associated with the atmospheric background can be rejected at the  $5.7\sigma$  level. If the observation of ultra-high energy cosmic rays revealed the existence of extreme cosmic accelerators, the IceCube neutrinos show that hadronic particle physics is in action in astrophysical sites at an energy scale somewhat higher than any man-made accelerator. IceCube is therefore opening a new window at the high-energy frontier of particle- and astro-physics. Motivated by this discovery we investigate here plausible  $\gamma$ -ray counterparts of the IceCube events

and discuss possible new scenarios. The detection of high-energy neutrinos up to the PeV ( $10^{15}$  eV) scale implies the existence of a class of astrophysical objects accelerating protons up to at least  $10^{16} - 10^{17}$  eV, which then collide with other protons ( $pp$  collisions) or photons ( $p\gamma$  collisions). High-energy  $\gamma$ -rays with energy and flux about a factor two higher than the neutrinos at the source, and therefore reaching the  $\gtrsim 60$  TeV range for the IceCube events, are also expected as secondary products in both cases (Kelner, Aharonian, & Bugayov 2006; Kelner & Aharonian 2008). In the following we refer to these  $\gamma$ -rays as neutrino *twins*. The study of these twin photons would provide the most direct way to shed light on the origin of the IceCube neutrinos. The twin photons, however, cannot be at the moment investigated due to the fact that present  $\gamma$ -ray telescopes reach only  $\sim 20 - 40$  TeV. Moreover, depending on the sources and their distance, absorption of the twin photons might dilute the direct photon-neutrino connection.

The topology of the IceCube detections are broadly classified in two types: 1. cascade-like, characterised by a compact spherical energy deposition; 2. track-like, defined by a dominant linear topology from the induced muon. A large majority of the 35 IceCube events are characterised by

\* E-mail: ppadovan@eso.org, elisa.resconi@tum.de

<sup>1</sup> <http://icecube.wisc.edu>

<sup>2</sup> In this paper neutrino means both neutrino and antineutrino.

a cascade-like topology, which, unlike the track-like topology, can only be reconstructed with a resolution in the tens of degrees. The association of the IceCube astrophysical neutrinos with astronomical sources is therefore not only limited by the missing twin photons but also by the relatively poor resolution of the events. Moreover, about half of the 35 events are expected to be background produced in the atmosphere (muons and neutrinos) and so mostly concentrated at lower energies.

IceCube has performed a series of tests on the incoming direction of the events showing no significant deviation from an assumed isotropic distribution nor prominent point sources. The all-sky integrated flux of neutrinos in the 60 TeV – 3 PeV range is at the level of  $10^{-8} \text{ GeV cm}^{-2} \text{ s}^{-1} \text{ sr}^{-1}$  per flavour for an  $E^{-2}$  spectrum. We note here that nearly half of the events reported by IceCube are on the Galactic plane (best fit position  $|b_{\text{ll}}| \leq 10^\circ$ ) with a few relatively close to the Galactic centre. The remaining half are at higher Galactic latitude. Hence both Galactic (e.g., Fox, Kashiyama, & Mészáros 2013; Taylor, Gabici, & Aharonian 2014) as well as extragalactic (e.g., Murase, Inoue, & Dermer 2014; Fang et al. 2014) scenarios provide valid explanations for the IceCube detections.

In this work we study  $\gamma$ -ray sources which fall within the median angular error of the IceCube events<sup>3</sup>. We refrain from modelling candidate sources and specific scenarios, addressing instead the question of the counterparts of the IceCube events from a purely phenomenological point of view by using the highest-energy all-sky catalogues. In the absence of photon observations above 60 TeV, in fact, we investigate possible counterparts in the GeV – TeV band. Each neutrino is studied independently as if it were a single detection in the sky. Both Galactic as well as extra-galactic sources are treated equally.

Section 2 defines the list of IceCube events adopted in this paper, while Section 3 describes the investigated  $\gamma$ -ray counterparts, their selection, and their  $\gamma$ -ray and neutrino *hybrid* spectral energy distributions (SEDs). Section 4 discusses our results, while in Section 5 we summarise our conclusions. We adopt here the definitions used in Aharonian (2004) for  $\gamma$ -ray astronomy: “high energy” (HE) or GeV astronomy spans the 30 MeV to 30 GeV energy range while “very high energy” (VHE) or TeV astronomy refers to the 30 GeV to 30 TeV range. For a review of VHE astronomy we refer to Holder (2012).

## 2 THE ICECUBE ASTROPHYSICAL NEUTRINOS

The first high-energy astrophysical neutrinos ever detected have been reported by IceCube through the selection of very high-energy events with interaction vertex inside the detector (IceCube Collaboration 2013). This containment strategy of very high-energy events is extremely efficient in rejecting the atmospheric background, including atmospheric neutrinos (Schönert et al. 2009). In doing so, the analysis

strategy favours cascade-like events, which deposit most of their energy inside the detector, over track-like ones, which travel various kilometres outside the detector. While, on the one hand, through the containment strategy astrophysical neutrinos are successfully singled out from the entire sky, on the other hand, the poor resolution of the cascade-like events makes the association with possible counterparts extremely challenging. Moreover, the absorption of very high-energy neutrinos crossing the Earth favours the southern hemisphere over the northern one, contrary to other IceCube analysis strategies optimized at lower energies, which are more sensitive to northern hemisphere events (Aartsen et al. 2013).

In order to reduce the residual atmospheric background contamination, which might still be produced by muons and atmospheric neutrinos and concentrate in the low-energy part of spectrum (see Fig. 2 in IceCube Collaboration 2014), we consider here only IceCube events with energy  $\geq 60$  TeV. Moreover, to somewhat limit the number of possible counterparts, we consider only events with median angular error  $\leq 20^\circ$ . These two cuts reduce the sample from 35 to 18 events. These are listed in Tab. 1, which gives the deposited energy of the neutrino, the flux at the deposited energy in  $\nu f_\nu$  units, the coordinates, the median angular error in degrees, the Galactic latitude, and the time of detection in Modified Julian Days. By interpreting each single event as coming from one astrophysical counterpart, in fact, we have derived the flux per neutrino event assuming that the observed flux is spread over 1 dex in energy and that the spectrum is  $f(\nu) \propto \nu^{-1}$  (equivalent to  $dN/dE \propto E^{-2}$ ). We use here an energy bin, which is somewhat larger than the IceCube average energy resolution. This is done to take into account the larger uncertainty due to the different topologies of the event and possible stochastic variations in the deposited energy of the single event. The resulting uncertainty in the flux estimate is almost fully absorbed in the Poissonian error and does not affect significantly the comparisons described in the following. Effective areas from the IceCube northern or southern hemisphere (depending on declination) and a live time of detection of 988 days (IceCube Collaboration 2014) were also used. In order to take into account the fact that the deposited energy is  $\sim 25\%$  lower than the neutrino energy, we have averaged the effective areas in two neighbouring bins (at the neutrino deposited energy and at the next highest one). The derived fluxes are in the range  $1.0 - 2.8 \times 10^{-11} \text{ erg cm}^{-2} \text{ s}^{-1}$  (i.e.,  $0.6 - 1.72 \times 10^{-8} \text{ GeV cm}^{-2} \text{ s}^{-1}$ ) and errors are Poissonian for one event (Gehrels 1986).

The 18 “golden” events are assumed here below to be all of astrophysical origin. They span a range of deposited energies from 60 TeV to 2 PeV, with a mean of  $\sim 350$  TeV. In  $pp$  or  $p\gamma$  collision scenarios (Kelner, Aharonian, & Bugayov 2006; Kelner & Aharonian 2008), the energy range of primary protons would be above a few tens of PeV. In primary cosmic rays, this is the region around and above the *knee*, which can be interpreted as the cross road of Galactic and extra-galactic cosmic rays (Giacinti, Kachelriess, & Semikoz 2014). Primary cosmic rays up to extremely high energies are significantly deviated by magnetic fields, hence the sources of these primary cosmic rays have not been identified yet. If the primary cosmic rays encounter enough target material, they inter-

<sup>3</sup> The IceCube Collaboration has reported up to now only the median angular error of their events.

**Table 1.** Selected list of high-energy neutrinos detected by IceCube.

IceCube ID	Dep. Energy TeV	$\nu f_\nu^a$ $10^{-11}$ erg/cm <sup>2</sup> /s	RA (2000)	Dec (2000)	median angular error deg	$b_{\text{II}}$ deg	Time (MJD)
3	$78.7^{+10.8}_{-8.7}$	$2.0^{+4.5}_{-1.6}$	08 31 36	−31 12 00	≤1.4	+5	55451.0707415
4	$165^{+20}_{-15}$	$1.1^{+2.6}_{-0.9}$	11 18 00	−51 12 00	7.1	+9	55477.3930911
5	$71.4 \pm 9.0$	$1.8^{+4.1}_{-1.5}$	07 22 24	−00 24 00	≤1.2	+7	55512.5516214
9	$63.2^{+7.1}_{-8.0}$	$2.8^{+6.5}_{-2.3}$	10 05 12	+33 36 00	16.5	+54	55685.6629638
10	$97.2^{+10.4}_{-12.4}$	$1.6^{+3.8}_{-1.4}$	00 20 00	−29 24 00	8.1	−65	55695.2730442
11	$88.4^{+12.5}_{-10.7}$	$1.5^{+3.4}_{-1.2}$	10 21 12	−08 54 00	16.7	+39	55714.5909268
12	$104 \pm 13.0$	$1.2^{+2.8}_{-1.0}$	19 44 24	−52 48 00	9.8	−29	55739.4411227
13	$253^{+26}_{-22}$	$1.6^{+3.7}_{-1.3}$	04 31 36	+40 18 00	≤1.2	−5	55756.1129755
14	$1041^{+132}_{-144}$	$1.6^{+4.3}_{-1.3}$	17 42 24	−27 54 00	13.2	−1	55782.5161816
17	$200 \pm 27$	$1.7^{+3.9}_{-1.4}$	16 29 36	+14 30 00	11.6	+38	55800.3755444
19	$71.5^{+7.0}_{-7.2}$	$1.8^{+4.1}_{-1.5}$	05 07 36	−59 42 00	9.7	−36	55925.7958570
20	$1141^{+143}_{-133}$	$1.5^{+3.5}_{-1.3}$	02 33 12	−67 12 00	10.7	−47	55929.3986232
22	$220^{+21}_{-24}$	$1.0^{+2.3}_{-0.8}$	19 34 48	−22 06 00	12.1	−19	55941.9757760
26	$210^{+29}_{-26}$	$1.5^{+3.5}_{-1.3}$	09 33 36	+22 42 00	11.8	−45	55979.2551738
27	$60.2 \pm 5.6$	$2.4^{+5.5}_{-2.0}$	08 06 48	−12 36 00	6.6	+10	56008.6845606
30	$129^{+14}_{-12}$	$1.1^{+2.6}_{-0.9}$	06 52 48	−82 42 00	8.0	−27	56115.7283566
33	$385^{+46}_{-49}$	$1.9^{+4.4}_{-1.6}$	19 30 00	+07 48 00	13.5	−5	56221.3423965
35	$2004^{+236}_{-262}$	$2.0^{+4.5}_{-1.6}$	13 53 36	−55 48 00	15.9	+6	56265.1338659

<sup>a</sup> Fluxes in units of  $10^{-8}$  GeV cm<sup>−2</sup> s<sup>−1</sup> can be obtained by multiplying the numbers in this column by 0.614.

act producing secondary neutrinos (from charged mesons) and photons (from neutral mesons). As photons and neutrinos are neutral they do not feel the effect of magnetic fields and can therefore be used in principle to probe astronomical PeV accelerators, the so-called PeVatrons.

### 3 THE COUNTERPARTS OF THE ICECUBE ASTROPHYSICAL NEUTRINOS

Neutrinos are intimately connected to their  $\gamma$ -ray counterparts. As a matter of fact, the twin photons coming from the same interactions that produced the IceCube neutrinos would have energies  $\gtrsim 120$  TeV and up to  $\sim 4$  PeV, and therefore well above the energy range of VHE astronomy. We will assume in the following a simple direct connection between VHE astronomical data and the  $\sim 100$  TeV – PeV band sampled by the IceCube data. Of course, the larger the gap between the highest photons detected and the IceCube neutrinos the more approximate such extrapolation becomes.

#### 3.1 $\gamma$ -ray catalogues

In order to alleviate the problem of the missing spectral coverage of the  $\gamma$ -rays twins of the IceCube neutrinos, our approach is to look for counterparts of the IceCube neutrinos in currently available all-sky catalogues that cover the highest possible energies. Namely, in decreasing order of energy and priority:

(i) TeVCat<sup>4</sup>, an online catalogue for VHE astronomy, which includes at the time of writing 147 sources detected typically above  $\approx 100$  GeV and reaching the TeV regime.

<sup>4</sup> <http://tevcat.uchicago.edu/>

Of these, 53 are blazars (50 BL Lacs and 3 flat-spectrum radio quasars [FSRQs]; see Sect. 3.2 for a description of the two blazar sub-classes) and 59 are Galactic sources, with the rest being mostly unclassified. TeVCat is a list of TeV sources, as there are no all-sky flux-limited TeV catalogues at the moment, given the very sparse sky coverage available at these energies. The High Energy Stereoscopic System (H.E.S.S.), however, has undertaken a TeV Galactic Plane survey covering a range of 250 to 65° in longitude at  $|b_{\text{II}}| < 3.5^\circ$  (Carrigan et al. 2013). There must be, therefore, many more TeV sources with fluxes comparable to the detected ones, which are still undetected, particularly at  $|b_{\text{II}}| > 3.5^\circ$ ;

(ii) the Wise High Synchrotron Peaked (WHSP) catalogue (Arsioli et al. 2014), which provides a large area ( $|b_{\text{II}}| > 20^\circ$ ) catalogue of  $\sim 1,000$  blazars and blazar candidates selected to have the peak of the synchrotron emission at  $\nu > 10^{15}$  Hz and therefore expected to radiate strongly in the HE and VHE bands. For our purposes we selected the sub-sample of 76 sources with a “figure of merit” (FoM) on their potential detectability in the TeV band  $\geq 1.2$ . The FoM is defined as the ratio between the synchrotron peak flux of a source and that of the faintest blazar in the WHSP sample already detected in the TeV band. The WHSP sources are all BL Lacs, with 39% of them being known TeV sources and the remaining ones thought to be within reach of detection by current VHE instrumentation. Although technically not a  $\gamma$ -ray catalogue, this WHSP sub-sample represents at present the best way to compensate for the lack of full sky coverage in the TeV band for blazars. Moreover,  $\sim 91\%$  of these sources have a *Fermi* 2FGL or 3FGL  $\gamma$ -ray counterpart (Arsioli et al. 2014);

(iii) the first *Fermi*-Large Area Telescope (LAT) catalogue of sources detected above 10 GeV (1FHL), which includes 514 sources,  $\sim 75\%$  of which are blazars (277 BL Lacs and 53 FSRQs) or blazar candidates (58) (Ackermann et al.

**Table 2.**  $\gamma$ -ray-detected blazars in one median angular error radius around the positions of the IceCube astrophysical neutrinos.

ID	Catalogue(s)	Counterpart(s)	RA (2000)	Dec (2000)	offset deg	$z$	$f_{10-500\text{GeV}}$ $10^{-12}$ c.g.s.	$f_{>200\text{GeV}}$ $10^{-12}$ c.g.s.	Type
4	1FHL	PKS 1101–536	11 04 15.4	−53 56 31	3.4	?	4.4	...	BL Lac
9	TeVCat/WHSP/1FHL	MKN 421	11 04 19.0	+38 11 41	12.8	0.031	319.8	100 – 500	BL Lac
	TeVCat/WHSP/1FHL	1ES 1011+496	10 15 04.0	+49 26 01	15.9	0.212	38.6	6.4	BL Lac
	WHSP/1FHL	B2 0912+29	09 15 54.0	+29 32 56	11.2	?	17.0	...	BL Lac
	1FHL	RX J0908.9+2311	09 09 21.4	+23 12 18	16.1	0.223	10.1	...	BL Lac
	1FHL	87GB 105148.6+222705	10 54 41.0	+22 14 02	15.7	?	5.8	...	BL Lac
	1FHL	RX J1100.3+4019	11 00 39.6	+40 18 54	12.9	0.225	5.8	...	BL Lac
	1FHL	Ton 1015	09 10 40.3	+33 33 18	11.3	?	4.9	...	BL Lac
	1FHL	RX J1023.6+3001	10 23 38.2	+29 59 42	5.3	0.433	4.6	...	BL Lac
	1FHL	1RXS J091211.9+275955	09 12 31.7	+27 58 26	12.6	?	4.1	...	BL Lac
	1FHL	B2 1040+24A	10 43 17.3	+24 07 08	12.6	0.559	3.1	...	BL Lac
	1FHL	S4 0917+44	09 20 55.2	+44 43 52	14.0	2.189	2.5	...	FSRQ
10	TeVCat/WHSP/1FHL	H 2356–309	23 59 09.0	−30 37 22	4.7	0.165	5.6	2.5	BL Lac
	1FHL	RBS 0016	00 08 46.6	−23 40 26	6.3	0.147	3.2	...	BL Lac
11	WHSP	1RXS J102244.2–011257	10 22 43.7	−01 13 02	7.7	0.369	8.1 <sup>a</sup>	...	BL Lac
	1FHL	PMN J0953–0840	09 52 57.1	−08 39 18	7.0	?	17.6	...	BL Lac
	1FHL	4C +01.28	10 58 30.7	+01 33 50	14.0	0.888	13.6	...	BL Lac
	1FHL	TXS 1013+054	10 16 02.4	+05 12 18	14.2	1.714	6.6	...	FSRQ
	1FHL	2FGL J1115.0–0701	11 15 02.4	−07 01 37	13.5	?	4.4	...	AGN <sup>b</sup>
	1FHL	BZB J1107+0222	11 07 30.7	+02 23 10	16.1	?	2.5	...	BL Lac
	1FHL	RXS J094620.5+010459	09 46 17.8	+01 06 18	13.3	0.557	2.2	...	BL Lac
	1FHL	PKS B1056–113	10 58 48.7	−11 34 12	9.6	?	2.0	...	BL Lac
12	TeVCat/WHSP/1FHL	PKS 2005–489	20 09 27.0	−48 49 52	5.6	0.071	39.6	6.7	BL Lac
	1FHL	PMN J1936–4719	19 36 51.4	−47 21 22	5.6	0.265	14.5	...	BL Lac
13	1FHL	4C +41.11	04 23 48.2	+41 51 04	2.1 <sup>c</sup>	?	14.8	...	BL Lac
14	1FHL	VERA J1823–3454	18 23 43.0	−34 55 08	11.3	?	19.4	...	?
	1FHL	PMN J1802–3940	18 02 43.2	−39 40 26	12.5	0.296	9.1	...	FSRQ
	1FHL	1RXS 182853.8–241746	18 28 59.0	−24 17 02	11.1	?	8.4	...	?
17	TeVCat/WHSP/1FHL	PG 1553+113	15 55 44.0	+11 11 41	8.9	?	146.7	4.5	BL Lac
	1FHL	2FGL J1548.3+1453	15 48 21.4	+14 55 19	10.0	?	4.2	...	? <sup>d</sup>
19	WHSP/1FHL	1RXS J054357.3–553206	05 43 55.4	−55 32 17	6.4	?	14.6	...	BL Lac
	1FHL	1ES 0505–546	05 06 55.2	−54 34 26	5.1	?	7.7	...	?
	1FHL	PKS 0516–621	05 16 37.9	−62 09 54	2.7	1.300	3.4	...	BL Lac
	1FHL	1RXS J043431.8–572718	04 34 08.9	−57 25 41	4.9	?	1.8	...	?
20	WHSP/1FHL	SUMSS J014347–584550	01 43 28.8	−58 44 56	10.1	?	11.2	...	BL Lac
	WHSP	PKS 0352–686	03 52 57.5	−68 31 17	7.6	0.087	...	...	BL Lac
	1FHL	1RXS J024439.8–581953	02 44 13.9	−58 13 08	9.1	0.265	6.9	...	BL Lac
22	WHSP <sub>low bII</sub> /1FHL	1H 1914–194	19 17 45.8	−19 21 54	4.8	0.137	19.2	...	BL Lac
	1FHL	PMN J1921–1607	19 22 00.2	−16 07 48	6.7	?	13.8	...	BL Lac
	1FHL	PKS 1958–179	20 01 06.7	−17 52 05	7.5	0.652	11.1	...	FSRQ
	1FHL	1RXS 195815.6–301119	19 58 24.2	−30 15 18	9.7	0.119	10.9	...	BL Lac
	1FHL	PMN J1911–1908	19 10 55.4	−19 06 14	6.3	?	10.9	...	?
26	WHSP/1FHL	B2 0912+29	09 15 54.0	+29 32 56	7.9	?	17.0	...	BL Lac
	WHSP	2MASXJ09260351+1243341	09 26 03.5	+12 43 34	10.1	0.186	...	...	BL Lac
	1FHL	RX J0908.9+2311	09 09 21.4	+23 12 18	5.6	?	10.1	...	BL Lac
	1FHL	MG1 J090534+1358	09 05 39.6	+13 59 10	10.9	?	9.3	...	BL Lac
	1FHL	OJ 287	08 54 50.9	+20 04 44	9.4	0.206	4.1	...	BL Lac
	1FHL	1RXS J091211.9+27595	09 12 31.7	+27 58 26	7.1	?	4.1	...	BL Lac
27	WHSP <sub>low bII</sub> /1FHL	PMN J0816–1311	08 16 21.8	−13 10 37	2.4	?	18.1	...	BL Lac
	1FHL	PKS 0805–07	08 08 16.8	−07 49 23	4.8	1.837	13.4	...	FSRQ
	1FHL	TXS 0815–094	08 18 01.7	−09 35 06	4.1	?	7.3	...	BL Lac
	1FHL	TXS 0752–116	07 54 23.8	−11 49 26	3.1	?	3.7	...	BL Lac
30	1FHL	PKS 1029–85	10 29 00.7	−85 43 48	5.9	?	3.1	...	BL Lac
	1FHL	PKS 0736–770	07 35 05.8	−77 08 13	5.8	?	3.0	...	BL Lac
33	1FHL	1RXS J193109.5+093714	19 31 04.8	+09 38 02	1.9	?	24.0	...	BL Lac
	1FHL	1RXS J194246.3+103339	19 42 52.1	+10 34 05	4.2	?	20.7	...	?
35	TeVCat	1ES 1312–423	13 14 58.0	−42 35 49	14.6	0.105	16.5	1.3	BL Lac
	1FHL	1RXS 130737.8–425940	13 07 43.0	−42 59 56	14.8	?	18.8	...	?
	1FHL	1RXS 130421.2–435308	13 04 19.2	−43 54 54	14.2	?	13.0	...	BL Lac
	1FHL	PKS B1424–418	14 28 02.9	−42 06 14	14.8	1.522	8.9	...	FSRQ
	1FHL	PMN J1234–5736	12 34 07.4	−57 35 31	11.0	?	7.3	...	?
	1FHL	PMN J1329–5608	13 28 46.8	−56 04 44	3.5	?	3.8	...	?
	1FHL	PMN J1326–5256	13 27 09.1	−52 58 26	4.8	?	3.6	...	BL Lac
	1FHL	PKS 1326–697	13 30 27.6	−70 05 02	14.5	?	2.2	...	?

<sup>a</sup> Flux in the 0.1 – 100 GeV range<sup>b</sup> AGN candidate (Ackermann et al. 2012)<sup>c</sup> Offset > median angular error<sup>d</sup> Blazar candidate (Massaro et al. 2013)

2013). The remaining objects are unclassified ( $\sim 13\%$ ) and Galactic ( $\sim 11\%$ ).

Our logic can be thus summarized: in the absence of VHE data reaching the  $\sim 100$  TeV – PeV band, we use TeVCat as our starting point. To compensate for its incompleteness and limited sky coverage we then add the WHSP catalogue, which however covers the high Galactic latitude sky and includes only blazars. Furthermore, as WHSP provides for most of its sources only a FoM for the TeV detectability, we complement it by using the highest energy *Fermi* catalogue, that is 1FHL, which gives an all-sky view above 10 GeV for all astronomical sources. As it turns out, the gap between 10 GeV and the neutrino energies ( $\geq 60$  TeV) appears to be quite large for a sensible extrapolation. Nevertheless, we wanted to be as thorough as possible in our search without penalizing sources, which have not been observed yet in the TeV band but might still one day prove to be plausible IceCube counterparts.

### 3.2 Blazar counterparts

Blazars are those Active Galactic Nuclei (AGN) whose emission is dominated by a relativistic jet viewed at a relatively small angle with respect to the line of sight (Urry & Padovani 1995). The two main blazar sub-classes, namely BL Lacertae objects (BL Lacs) and FSRQs, differ mainly in their optical spectra, with the former displaying strong, broad emission lines and the latter instead being characterized by optical spectra showing at most weak emission lines, sometimes exhibiting absorption features, and in many cases being completely featureless (see Giommi et al. 2012; Giommi, Padovani, & Polenta 2013, for a recent re-evaluation of the two blazar classes). The strong non-thermal blazar radiation, which spans the entire electromagnetic spectrum, is composed of two broad humps, the low-energy one attributed to synchrotron radiation, and the high-energy one, usually thought to be due to inverse Compton radiation (see e.g. Abdo et al. 2010) or, alternatively, to hadronic processes (e.g. Böttcher et al. 2013, and reference therein). The peak of the synchrotron hump,  $\nu_{\text{peak}}$ , ranges from about  $\sim 10^{12.5}$  Hz to over  $10^{18}$  Hz reflecting the maximum energy at which particles can be accelerated (e.g. Giommi et al. 2012). Blazars with  $\nu_{\text{peak}} < 10^{14}$  Hz in their rest frame are called Low Synchrotron Peaked (LSP) sources, while those with  $10^{14}$  Hz  $< \nu_{\text{peak}} < 10^{15}$  Hz, and  $\nu_{\text{peak}} > 10^{15}$  Hz are called Intermediate and High Synchrotron Peaked (ISP and HSP) sources respectively (Abdo et al. 2010). This definition extends the original division of BL Lacs into LBL and HBL sources first introduced by Padovani & Giommi (1995). Basically all HSP are BL Lacs (see Giommi et al. 2012; Padovani, Giommi, & Rau 2012, for a possible explanation). Objects with large  $\nu_{\text{peak}}$  are obviously favoured to be VHE sources. Indeed, only one out of the fifty currently TeV-detected BL Lacs is an LSP.

Due to their very large luminosities and SEDs routinely reaching the HE and VHE bands, blazars are thought to be amongst the most powerful accelerators in the Universe and as a result have been considered prime candidate sources of ultra-high energy cosmic rays and neutrinos (Halzen & Vazquez 1993; Protheroe 1997; Mannheim 1999; Dermer & Atoyan 2001).

Tab. 2 shows the results of our search for blazars and gives the IceCube ID, the catalogues where the counterparts were found, the counterparts’ names and coordinates, ranked by energy (TeVCat first) and flux, the offset between the reconstructed position of the IceCube event and the blazar one, the redshift of the source (if available), the 10 – 500 GeV flux (from the 1FHL catalogue), the (observed) flux above 200 GeV (from papers referenced in TeVCat) for the TeV-detected sources, and the blazar type, namely BL Lac, FSRQ, or unknown<sup>5</sup>. Note that given the very strong variability of blazars flux values should be taken only as approximate. Nevertheless, fluxes are important as, on average, a stronger neutrino source should also be a stronger  $\gamma$ -ray source, unless significant absorption is present (Sect. 1).

Blazar counterparts were found for 16/18 neutrino events, in one case (ID 13) with an offset slightly larger ( $\sim 1.8$  times) than the median angular error. Namely, six (with two sources correlated with the same event) were found in TeVCat (all of them in 1FHL), eleven are WHSP sources (nine of which are in 1FHL as well), while all others were found in 1FHL.

We stress that 8/9 of the IceCube events with  $|b_{\text{II}}| > 20^\circ$  have WHSP counterparts. Even more strikingly, and as is the case for TeVCat, in all these cases the WHSP source(s) is (are) always the strongest one(s). This vindicates the use of a selection on synchrotron peak and flux to identify present or potential TeV emitters and is particularly important for events without TeVCat counterparts, namely ID 11, 19, 20, and 26. We also note that the strongest 1FHL counterpart of ID 22, 1H 1914–194, which has  $|b_{\text{II}}| < 20^\circ$  and therefore is not included by definition in WHSP, fulfills the other criteria ( $\nu_{\text{peak}}$  and FoM) and therefore is a very promising TeV candidate. Same story for PMNJ0816–1311, the strongest 1FHL counterpart of ID 27<sup>6</sup>. We have therefore marked these two sources as WHSP<sub>low  $b_{\text{II}}$</sub>  in Tab. 2.

Tab. 2 includes some well-known, bright BL Lacs, i.e., MKN 421, PKS 2005–489, PG 1553+113. Only three sources, namely B2 0912+29, RX J0908.9+2311, and 1RXS J091211.9+275955, are associated with more than one neutrino event (ID 9 and 26). Out of the 61 unique objects in Tab. 2 only six are FSRQs, with none of them being the strongest source within the error circle. Most ( $\sim 88\%$ ) neutrino events have more than one blazar counterpart.

For the two neutrino events for which no counterpart was found in the three catalogues used, we checked for completeness the *Fermi*-2FGL catalogue (Nolan et al. 2012), which includes 1,873 sources detected above 100 MeV<sup>7</sup>. In both cases we found a counterpart: 2FGL J0825.9–3216 (PKS 0823–321, an AGU), with an offset of  $1.6^\circ$  (slightly above the median angular error) for ID 3 and 2FGL J0726.0–0053 (PKS 0723–008, an other AGU), with an off-

<sup>5</sup> This refers to the so-called “active galaxies of uncertain type” (AGU), most of which are expected to be blazars (e.g. Ackermann et al. 2013).

<sup>6</sup> We thank Paolo Giommi for pointing this out to us.

<sup>7</sup> The 2FGL includes blazars or blazar candidates ( $\sim 59\%$ ), Galactic ( $\sim 10\%$ ) and unclassified ( $\sim 31\%$ ) sources.

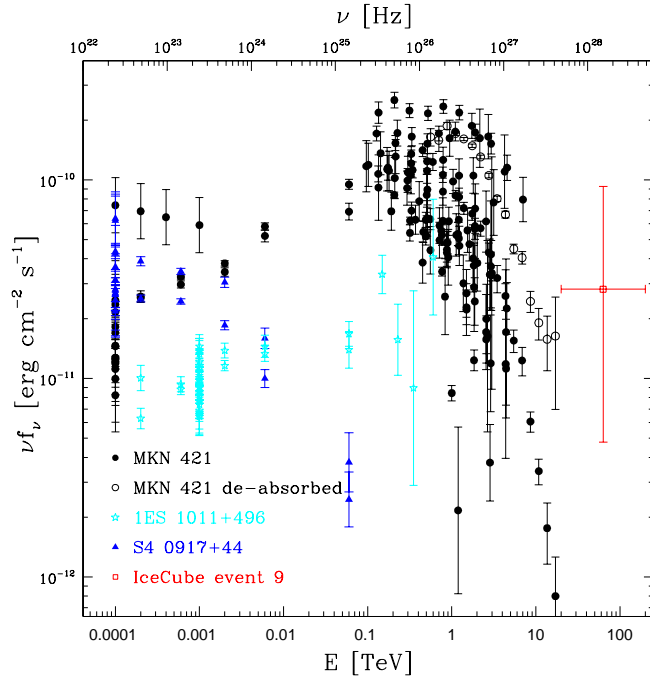


**Figure 1.**  $\gamma$ -ray SED of MKN 421 (black filled circles) and the HEGRA data (Aharonian et al. 2002) corrected for absorption by the EBL (black open circles) (Franceschini, Rodighiero, & Vaccari 2008), 1ES 1011+496 corrected for absorption by the EBL (cyan stars), and S4 0917+44 (blue triangles), respectively the strongest, second strongest, and weakest sources in the IceCube error circle (ID 9). The many data points for MKN 421 represent different states of the source. The (red) open square represents the neutrino flux for the corresponding IceCube event; vertical error bars are Poissonian for one event, while the horizontal one indicates the range over which the flux is integrated.

set of  $1^\circ$  for ID 5. For both objects the HE emission reaches  $\sim 6$  GeV, i.e. not too far from the 1FHL cutoff.

### 3.2.1 Hybrid SEDs

To see how the neutrino and photon energetics compare, we have put together the  $\gamma$ -ray SEDs of all sources using the SED builder<sup>8</sup> of the ASI Science Data Centre (ASDC) adding, if needed, VHE data taken from the literature. We have also included the flux per neutrino event at the specific energy, thereby building a hybrid photon – neutrino SED. We then performed an “energetic” diagnostic by checking if a simple extrapolation succeeded in connecting the most energetic  $\gamma$ -rays to the IceCube neutrino in the hybrid SED, taking into account the rather large uncertainty in the flux of the latter. If this was the case we considered the source to be a probable counterpart. Otherwise, we discarded the object. Anything more sophisticated would require detailed modelling, which goes beyond the scope of this paper. We show in Figs. 1 – 4 and Fig. 8 the SEDs of the TeV-detected blazars, which we now turn to comment:

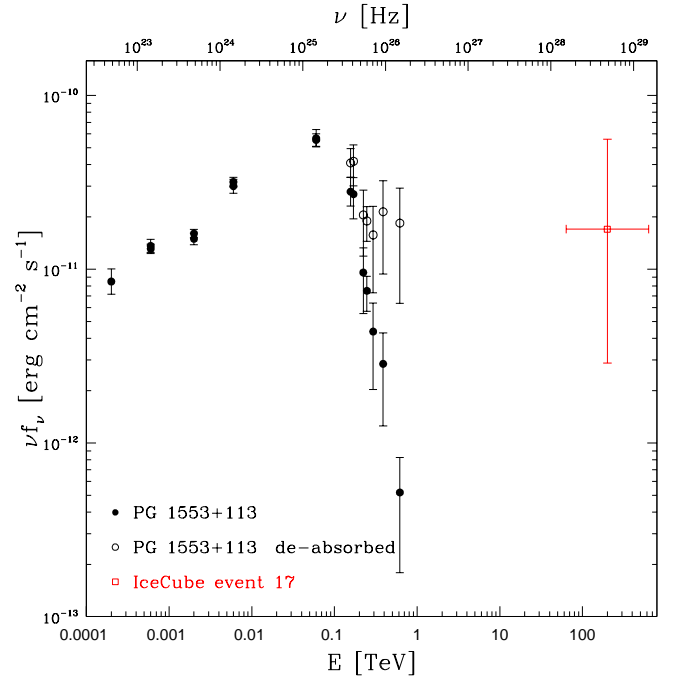


**Figure 2.**  $\gamma$ -ray SED of PG 1553+113: observed (black filled circles) and corrected for absorption by the EBL (black open circles) assuming  $z = 0.4$  (Aleksić et al. 2012). The (red) open square represents the neutrino flux for the corresponding IceCube event (ID 17); error bars as described in Fig. 1.

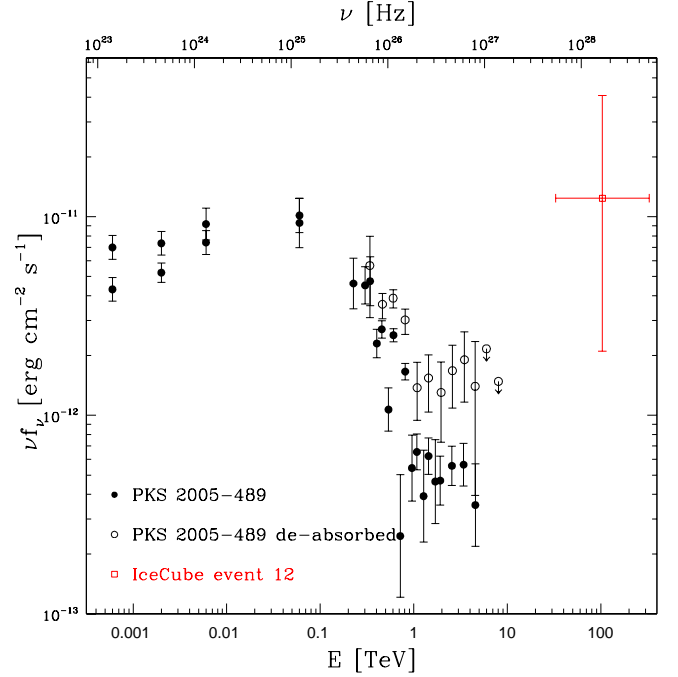


**Figure 3.**  $\gamma$ -ray SED of PKS 2005-489: observed (black filled circles) and corrected for absorption by the EBL (black open circles) (Şentürk et al. 2013). The (red) open square represents the neutrino flux for the corresponding IceCube event (ID 12); error bars as described in Fig. 1.

<sup>8</sup> <http://tools.asdc.asi.it/SED/>

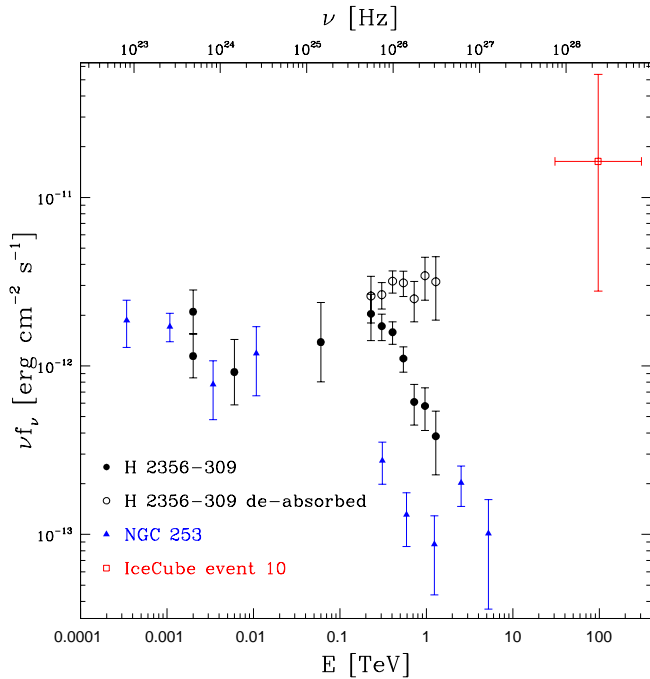


**Figure 4.**  $\gamma$ -ray SED of H 2356-309: observed (black filled circles) and corrected for absorption by the EBL (black open circles) (Costamante 2012). The SED of NGC 253 (blue triangles) is also shown (Abramowski et al. 2012). The (red) open square represents the neutrino flux for the corresponding IceCube event (ID 10); error bars as described in Fig. 1.

- MKN 421<sup>9</sup> (Fig. 1); this is the strongest  $\gamma$ -ray source in our sample and a simple extrapolation of its VHE spectrum has no problems in explaining the energy and flux of the corresponding IceCube event (ID 9), even taking into account the factor  $\sim 2$  increase expected for the energy and flux of the twin photons associated with the neutrinos. This is a clear case that passes the “energetic” diagnostic. Fig. 1 shows also the SED, corrected for absorption by the extragalactic background light (EBL), of 1ES 1011+496, the other TeVCat BL Lac in the same error circle, which appears also to be a plausible counterpart. Finally, the SED of S4 0917+44, which is the weakest source amongst the other nine blazars associated with ID 9, is also displayed. While the  $\gamma$ -ray spectra of MKN 421 and 1ES 1011+496 are raising with energy, that of S4 0917+44 is falling, which makes it a very unlikely counterpart for the IceCube event. This shows how important the “energetic” diagnostic is, especially because of the relatively loose spatial one, given the large error circles. We note that, for our purposes, the extrapolation to  $\gamma$ -ray energies larger than the observed ones is not influenced by the EBL as neutrinos reflect the photon densities *at the source* and not at the observer after the interaction with the EBL photons. However, the comparison between observed photon and neutrino fluxes is affected, as the former will be absorbed by the EBL, above  $\approx 100$  GeV, while the latter will not;

- PG 1553+113 (Fig. 2); in this case the EBL has a very

<sup>9</sup> Fang et al. (2014) have compared the TeV flux of MKN 421 and the neutrino fluxes related to ID 9.

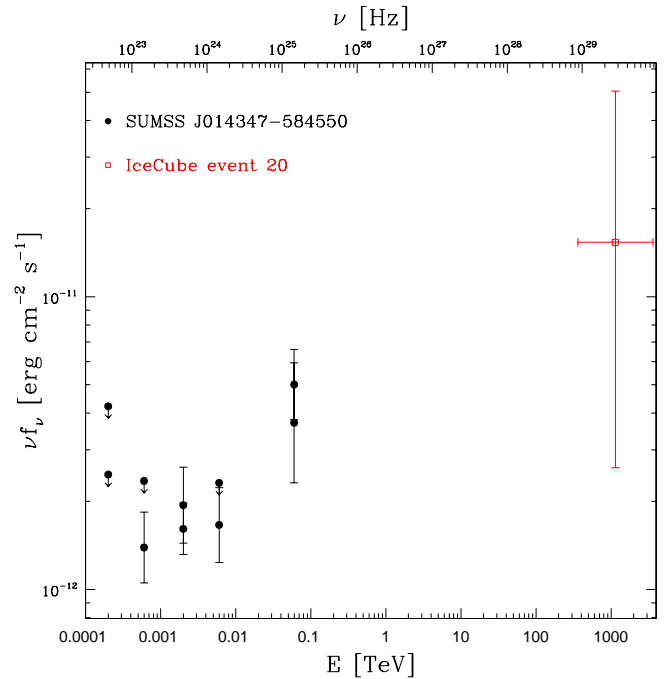


**Figure 5.**  $\gamma$ -ray SED of SUMSS J014347-584550 (black filled circles). The (red) open square represents the neutrino flux for the corresponding IceCube event (ID 20); error bars as described in Fig. 1.

strong effect and, after correcting for its absorption (assuming  $z = 0.4$ : see discussion in Aleksić et al. 2012), its VHE spectrum appears also consistent with the IceCube event (ID 17);

- PKS 2005-489 (Fig. 3); despite being relatively local, the EBL has an effect also on the VHE spectrum of this BL Lac, which reaches relatively large energies ( $\sim 5$  TeV). However, even taking this into account, its VHE spectrum appears to be inconsistent with a neutrino detection (ID 12);

- H 2356-309 (Fig. 4); the EBL has quite a strong effect also on the VHE spectrum of this BL Lac and, after correcting for it, its VHE spectrum appears consistent with the IceCube event (ID 10).

We point out that also some of the 1FHL blazars in Tab. 2 display SEDs, which appear at a first glance not inconsistent with the corresponding neutrino event. However, the gap between the highest observable energy and that of the neutrino is much ( $\sim 10 - 100$  times) larger than that typical of TeV-detected sources, making any possible neutrino – photon association harder to pin down. We make an exception for WHSP sources, for which we have very strong hints of a possible TeV emission. As an example, we show in Fig. 5 the SED of SUMSS J014347-584550, a WHSP source and the strongest counterpart of ID 20 (one of the three PeV events). A simple extrapolation of the HE spectrum appears not inconsistent with the energy and flux of the corresponding IceCube event, given its rising SED. The same argument applies to 1RXS J054357.3-553206 (ID 19), 1H 1914-194 (ID 22) and PMN J0816-1311 (ID 27).

We present our list of the most plausible counterparts in Sect. 4.

**Table 3.**  $\gamma$ -ray-detected non-blazars in one median angular error radius around the positions of the IceCube astrophysical neutrinos.

ID	Catalogue	Counterpart(s)	RA (2000)	Dec (2000)	offset deg	$f_{10-500\text{GeV}}$ $10^{-12}$ c.g.s.	flux Crab	Class <sup>a</sup>
10	TeVCat	NGC 253	00 47 34	−25 17 22	7.4	0.6 <sup>b</sup>	0.0021	<b>Starburst</b>
14 <sup>c</sup>	TeVCat	HESS J1804−216	18 04 31	−21 41 60	8.0	...	0.25	extended
	TeVCat	HESS J1809−193	18 10 31	−19 18 00	10.7	...	0.14	PWN
	TeVCat	HESS J1813−178	18 13 36	−17 50 24	12.4	...	0.06	PWN
	TeVCat	HESS J1745−303	17 45 02	−30 22 12	2.5	...	0.05	SNR/Molec
	TeVCat/1FHL	Galactic Centre	17 45 39	−29 00 22	1.3	30.2	0.05	unidentified
	TeVCat	CTB 37A	17 14 19	−38 34 00	12.2	...	0.03	SNR/Molec
	TeVCat	HESS J1718−385	17 18 07	−38 33 00	11.8	...	0.02	PWN
	TeVCat	HESS J1741−302	17 41 00	−30 12 00	2.3	...	0.01	unidentified
	TeVCat	G0.9+0.1	17 47 23	−28 09 06	1.1	...	0.02	PWN
	TeVCat	CTB 37B	17 13 57	−38 12 00	11.9	...	0.018	Shell
	TeVCat	Terzan 5	17 47 49	−24 48 30	3.3	...	0.015	Globular
	TeVCat/1FHL	SNR G349.7+0.2	17 18 01	−37 26 30	10.8	19.9	0.004	SNR/Molec
	TeVCat	HESS J1729−345	17 29 35	−34 32 22	7.2	...	...	extended
	TeVCat	HESS J1731−347	17 32 03	−34 45 18	7.2	...	...	Shell
	TeVCat	HESS J1800−240C	17 58 51	−24 03 07	5.3	...	...	SNR/Molec
	TeVCat	HESS J1800−240B	18 00 26	−24 02 20	5.6	...	...	SNR/Molec
	TeVCat/1FHL	W28	18 01 42	−23 20 06	6.3	46.3	...	SNR/Molec
	TeVCat	HESS J1800−240A	18 01 57	−23 57 43	5.9	...	...	SNR/Molec
	TeVCat	HESS J1808−204	18 08 00	−20 24 00	9.5	...	...	unidentified
	1FHL	PWN G0.13−0.11	17 46 22	−28 51 47	1.3	30.2	...	PWN
	1FHL		17 58 22	−23 40 16	5.5	12.9	...	unidentified
	1FHL	LAT PSR J1809−2332	18 09 51	−23 29 46	7.6	10.1	...	HPSR
	1FHL		17 41 56	−25 39 29	2.2	7.7	...	unidentified
19	1FHL	Large Magellanic Cloud	05 26 36	−68 25 12	9.0	38.8	...	<b>Galaxy</b>
	1FHL		05 09 56	−64 19 44	4.6	3.5	...	unidentified
27	1FHL		08 04 53	−06 26 06	6.2	2.3	...	unidentified
33	TeVCat/1FHL	MGRO J1908+06	19 07 54	+06 16 07	5.7	5.1	0.17	PWN <sup>d</sup>
	TeVCat	HESS J1912+101	19 12 49	+10 09 06	4.9	...	0.1	PWN
	TeVCat/1FHL	W51	19 22 55	+14 11 27	6.6	55.2	0.03	SNR/Molec
	TeVCat	G54.1+0.3	19 30 32	+18 52 12	11.1	...	0.025	PWN
	TeVCat	IGR J18490−0000	18 49 01	−00 01 17	12.9	...	0.015	PWN
	TeVCat/1FHL	W49B	19 11 06	+09 05 34	4.8	27.7	0.005	SNR/Molec
	TeVCat/1FHL	HESS J1857+026	18 57 11	+02 40 00	9.6	64.2	...	extended
	TeVCat	HESS J1858+020	18 58 20	+02 05 24	9.7	...	...	extended
	1FHL	SNR G034.7−00.4	18 55 58	+01 21 18	10.6	27.3	...	SNR
35	TeVCat	HESS J1303−631	13 02 48	−63 10 39	9.8	...	0.17	PWN
	TeVCat	MSH 15−52	15 14 07	−59 09 27	11.3	...	0.15	PWN
	TeVCat	HESS J1356−645	13 56 00	−64 30 00	8.7	...	0.11	PWN
	TeVCat	RCW 86	14 42 42	−62 26 41	9.1	...	0.1	Shell
	TeVCat	PSR B1259−63	13 02 49	−63 49 53	10.2	...	0.07	Binary
	TeVCat/1FHL	Kookaburra J1420−607	14 20 09	−60 45 36	6.1	31.8 (23.4 <sup>b</sup> )	0.07	PWN
	TeVCat/1FHL	Kookaburra J1418−609	14 18 04	−60 58 31	6.1	12.1 (17.4 <sup>b</sup> )	0.06	PWN
	TeVCat	HESS J1458−608	14 58 09	−60 52 38	9.8	...	0.06	PWN
	TeVCat	HESS J1503−582	15 03 38	−58 13 45	9.8	...	0.06	DARK
	TeVCat/1FHL	HESS J1507−622	15 06 52	−62 21 00	11.4	9.0	0.01	extended
	TeVCat/1FHL	Centaurus A	13 25 26	−43 00 42	13.6	6.1 (1.7 <sup>b</sup> )	0.008	<b>Radio galaxy</b>
	TeVCat	HESS J1427−608	14 27 52	−60 51 00	6.8	...	...	extended
	TeVCat	G318.2+0.1	14 57 46	−59 28 00	9.3	...	...	SNR/Molec
	1FHL		14 07 12	−61 33 40	6.0	21.3	...	unidentified
	1FHL		13 28 35	−47 28 16	9.2	9.1	...	unidentified
	1FHL	LAT PSR J1413−6205	14 13 25	−62 05 53	6.8	8.8	...	HPSR
	1FHL		13 53 05	−66 42 43	10.9	6.8	...	unidentified
	1FHL	PSR J1514−4946	15 14 20	−49 45 04	13.6	3.2	...	HPSR

<sup>a</sup> Binary:  $\gamma$ -ray binary; DARK: no associations in other bands; extended: unclassified Galactic source; Globular: globular cluster; HPSR: Pulsar identified by pulsations above 10 GeV; PWN: pulsar wind nebula; Shell: shell-type supernova remnant; SNR: supernova remnant; SNR/Molec: supernova remnant/molecular cloud

<sup>b</sup> Flux at energies  $> 200$  GeV

<sup>c</sup> Event consistent with the position of the Galactic centre

<sup>d</sup> Acero et al. (2013)



### 3.3 Non-blazar counterparts

Alternative scenarios for PeV neutrino sources beyond the blazar one include  $\gamma$ -ray bursts (GRB) (Asano & Mészáros 2014, and references therein), supernovae remnants (Villante & Vissani 2008, and references therein), pulsar wind nebulae (PWN; Bednarek 2003), and star-forming galaxies (Tamborra, Ando, & Murase 2014, and references therein). At present, the IceCube Collaboration reports no evidence of a GRB – neutrino connection (Abbasi et al. 2012), although this not based on the same events considered here.

The non-blazar counterparts present in the catalogues studied in this work are listed in Tab. 3, where we give also the 10 – 500 GeV flux (from the 1FHL catalogue) and the HE flux in Crab units (as provided by TeVCat), if available. Sources were found for six neutrino events, four of them on the Galactic plane ( $|b_{\text{II}}| \leq 10^\circ$ ) and one of which actually consistent with the position of the Galactic centre. The error circles of the two events off the Galactic plane include one and two non-blazar counterparts respectively: NGC 253, a starburst galaxy (ID 10), and the Large Magellanic Cloud (LMC) plus an unidentified source (ID 19). While NGC 253 and the unidentified source have fluxes  $\sim 4$  times smaller than those of the brightest blazars in the same error circle, this is not the case for the LMC, which is  $\sim 2.6$  times brighter than 1RXS J054357.3–553206, which however is a WHSP source. ID 27 has a single, weak non-blazar counterpart which, being an unidentified 1FHL source, might be a blazar as well. For the other three events we found a very large number ( $\sim 10 - 20$ ) of counterparts, many with fluxes larger than those of the blazar counterparts. For example, Kookaburra J1420–607, a PWN associated with ID 35 has a flux above 200 GeV  $\sim 20$  times larger than that of 1ES 1312–423, the BL Lac in the same error circle in TeVCat. And two supernova remnants associated with ID 14 and 33 have a 10 – 500 GeV flux  $\sim 2.5$  times larger than the respective brightest associated BL Lacs. We address in more detail the comparison between blazar and non-blazar counterparts in Sect. 3.3.1.

We note that of the thirty-seven classified sources in Tab. 3 all but three are Galactic, the exceptions being (highlighted in bold face in the table) the LMC, NGC 253, mentioned above, and Centaurus A, a radio galaxy associated with ID 35. This latter source is particularly interesting in this respect as the region around it is populated by a number of ultra high-energy cosmic ray events larger than the rest of the sky, although recent results show a chance probability for this to occur at a level of  $\sim 4\%$  (Kampert et al. 2012). However, we point out that, amongst the many  $\gamma$ -ray sources in the error circle of ID 35, Centaurus A is one of the weakest.

#### 3.3.1 Hybrid SEDs

As done for blazars, we have put together the hybrid SEDs of all sources. It turned out that only two Galactic sources passed the “energetic” diagnostic being actually better at that than the blazars in the same error circle. We show here some of the most promising Galactic counterparts of the IceCube events.

Fig. 6 shows the  $\gamma$ -ray SEDs of three sources in the error

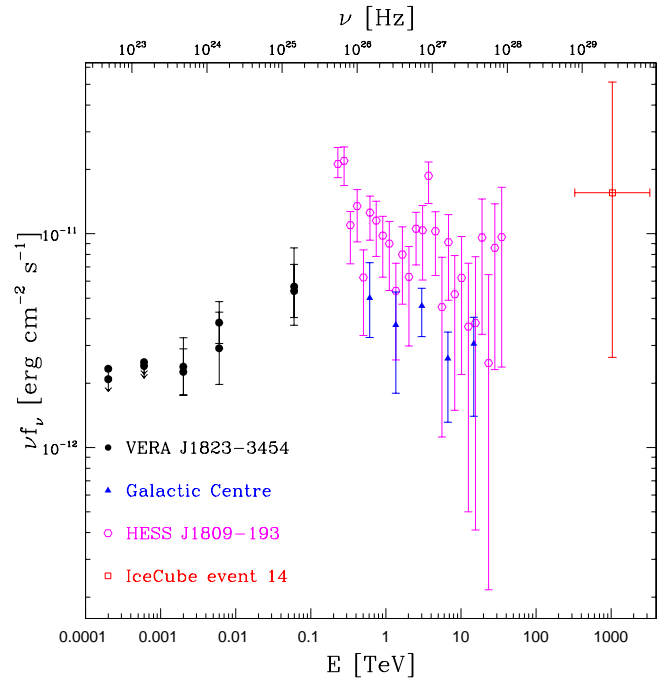


**Figure 6.**  $\gamma$ -ray SEDs of three sources in the error circle of ID 14, namely: the BL Lac VERA J1823–3454 (black filled circles), the PWN HESS J1809–193 (magenta hexagons) (Renaud et al. 2008) and the Galactic Centre (Aharonian et al. 2004). The (red) open square represents the neutrino flux for the corresponding IceCube event; error bars as described in Fig. 1.

circle of ID 14, namely VERA J1823–3454, the strongest blazar, HESS J1809–193, the second strongest TeV source and a PWN, and the Galactic Centre. The latter two reach  $\sim 20 - 40$  TeV but only HESS J1809–193 seems to be a plausible astronomical counterpart, since the Galactic Centre appears to be too soft. The BL Lac has a strongly rising SED but reaches only  $\sim 60$  GeV, which makes any extrapolation to the PeV range very uncertain.

Fig. 7 shows the  $\gamma$ -ray SEDs of three sources in the error circle of ID 33, namely 1RXS J193109.5+093714, the strongest BL Lac, MGRO J1908+06, the strongest TeV source and a PWN, and HESS J1857+026, an extended Galactic source. The latter two both reach  $\sim 20 - 40$  TeV. However, only MGRO J1908+06 seems to be a plausible astronomical counterpart, since HESS J1857+026 appears to be too soft. The BL Lac reaches only  $\sim 60$  GeV with an upper limit at  $\sim 1$  TeV a factor of 3 below the fluxes of the two Galactic sources.

Fig. 8 shows the  $\gamma$ -ray SEDs of four sources in the error circle of ID 35, which is the IceCube event with the largest energy ( $\sim 2$  PeV). These include: 1ES 1312–432, the only blazar in TeVCat, Centaurus A, and two PWNs, HESS J1356–645 and Kookaburra J1418–609. The PWNs are more than one order of magnitude brighter than the two extragalactic ones at  $E > 1$  TeV but still appear to fail the “energetic” test. We therefore cannot match the most energetic IceCube event with a plausible astronomical counterpart. However, as discussed in Sec. 3.2.1, we cannot exclude that one of the 1FHL sources in the same error box is a TeV emitter and responsible for the neutrino emission.

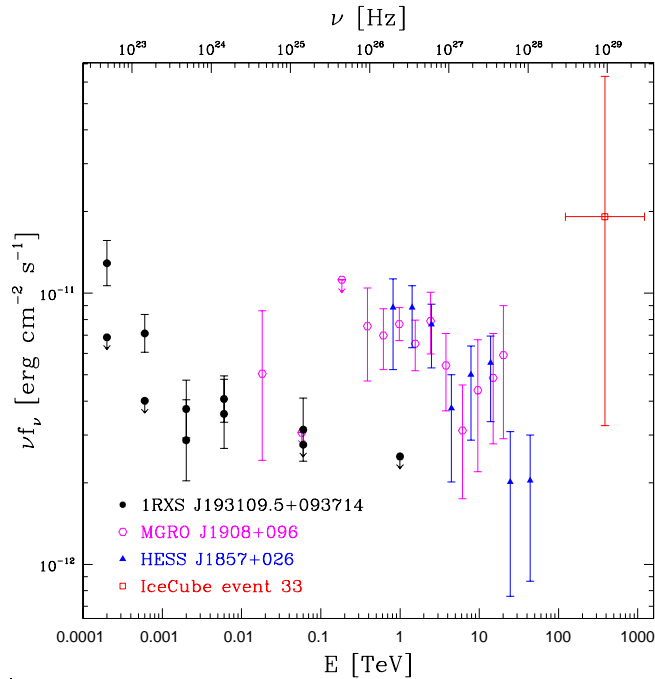


**Figure 7.**  $\gamma$ -ray SEDs of three sources in the error circle of ID 33, namely: the BL Lac 1RXS J193109.5+093714 (black filled circles) and the Galactic sources MGRO J1908+06 (magenta hexagons) (Acero et al. 2013, and references therein) and HESS J1857+026 (blue triangles) (Aharonian et al. 2008). The (red) open square represents the neutrino flux for the corresponding IceCube event; error bars as described in Fig. 1.

Note that in the case of the radio galaxy and the BL Lac the EBL does not make much of a difference: Centaurus A is at  $z = 0.002$  while the correction for 1ES 1312–432, which has a redshift in between those of PKS 2005–489 and H 2356–309 ( $z = 0.105$ ), will therefore be between a factor  $\sim 3$  and  $\sim 10$  (see Figs. 3 and 4). Interestingly, the predicted neutrino flux from Centaurus A at the energy of ID 35 is  $\approx 1,000$  times smaller than the flux connected with that event (Saba, Tjus, & Halzen 2013).

In Fig. 4 we plot the  $\gamma$ -ray SED of NGC 253 as well, a starburst galaxy also in the error circle of ID 10. As could be anticipated by its relatively low VHE flux, the SED drops steeply and clearly fails the “energetic” diagnostic. Given its very low redshift ( $z = 0.0008$ ) the effect of the EBL is negligible and therefore NGC 253 is an extremely unlikely counterpart of the IceCube event. As was the case for Centaurus A, a very recent paper by Yoast-Hull et al. (2014) predicts for NGC 253 a neutrino flux at the energy of ID 10  $\approx 2,000$  times smaller than the flux connected with that event. We present our list of most plausible counterparts in Sect. 4.

#### 4 DISCUSSION

Our goal was to investigate the origin of the first high-energy astrophysical neutrinos ever detected through a model independent approach. The most natural sources to begin with are  $\gamma$ -ray emitters. Starting from Tab. 2 and 3, we have studied the photon – neutrino hybrid SEDs of all

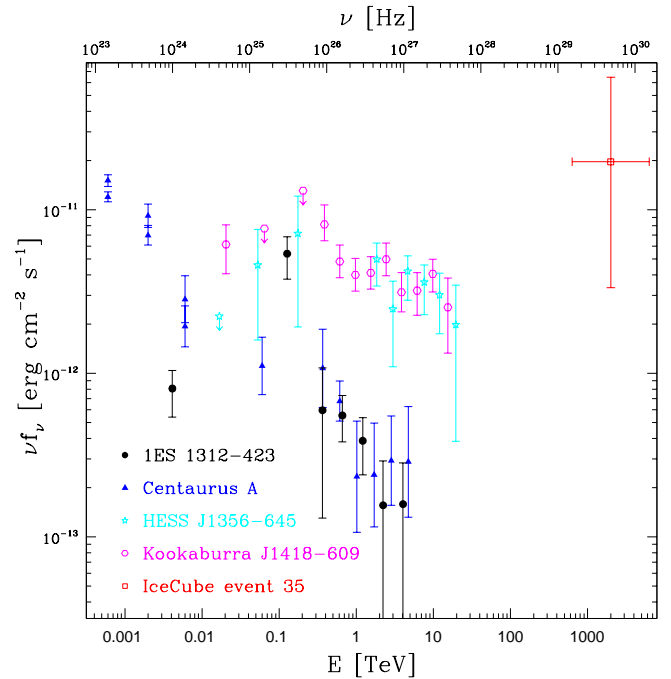


**Figure 8.**  $\gamma$ -ray SEDs of four sources in the error circle of ID 35, namely: the BL Lac 1ES 1312–432 (black filled circles) (HESS Collaboration et al. 2013), the radio galaxy Centaurus A (blue triangles), and the PWNe HESS J1356–645 (cyan stars) and Kookaburra J1418–609 (magenta hexagons) (Acero et al. 2013, and references therein). The (red) open square represents the neutrino flux for the corresponding IceCube event; error bars as described in Fig. 1.

possible counterparts. This turned out to be a very powerful discriminant for the likelihood of the association, especially given the relatively large error circles of the neutrino detections.

In the comparisons presented in Fig. 1 to Fig. 8, a gap is present typically from  $\approx 10 - 30$  TeV to (neutrino) energies  $\gtrsim 100$  TeV (apart from Fig. 5 where the gap is much larger). Any possible extrapolation to close such a gap is highly non trivial. Moreover, strong variability and different emission peak energies displayed by blazars complicate even further the matter. We have nevertheless singled out  $\gamma$ -ray sources, which we believe are plausible counterparts.

Only 10% (6/47) of the TeVcat counterparts passed the “energetic” test, the others being too  $\gamma$ -ray faint. In order to make up for the rather scanty sky coverage of TeV-Cat, particularly in the high-latitude sky, we have also taken into consideration the WHSP blazars still not TeV-detected, applying the “energetic” test to them as well but considering in this case the strong likelihood that they might be TeV emitters. This way we singled out four WHSP-only objects and ranked them as probable counterparts. The 1FHL-only sources, although in some cases intriguing from the energetic side, turned out to have too large of a gap between their highest electromagnetic energy and that of the IceCube event to make a sensible link between photons and neutrinos. Moreover, without even a hint of a possible emission in the VHE band, we decided not to rank in this work the 1FHL-only sources as probable candidates.

Our findings are summarized in Tab. 4, which gives

**Table 4.** List of most probable counterparts of selected IceCube high-energy neutrinos.

IceCube ID	Counterpart(s)	Class	Catalogue(s)
9	MKN 421	BL Lac (HSP)	TeVCat/WHSP
	1ES 1011+496	BL Lac (HSP)	TeVCat/WHSP
10	H 2356–309	BL Lac (HSP)	TeVCat/WHSP
14	HESS J1809–193	PWN	TeVCat
17	PG 1553+113	BL Lac (HSP)	TeVCat/WHSP
19	1RXS J054357.3–553206	BL Lac (HSP)	WHSP
20	SUMSS J014347–584550	BL Lac (HSP)	WHSP
22	1H 1914–194	BL Lac (HSP)	WHSP
27	PMN J0816–1311	BL Lac (HSP)	WHSP
33	MGRO J1908+06	PWN	TeVCat

the most probable neutrino counterparts for 9/18 of the IceCube events. We stress that this does not mean that the remaining nine events have no astronomical counterparts but rather that there is less information available for the sources in their error circles for us to be able to judge on their association likelihood.

The counterparts turned out to be mostly HSP BL Lacs and two PWNe, pushing forward a mixed scenario of Galactic and extra-galactic neutrino sources, so far not yet considered in the literature. We note that one of the three PeV events (ID 14) appears to have only one plausible counterpart, a Galactic one. The second PeV IceCube event (ID 20) has one WHSP BL Lac counterpart but no Galactic ones, while the third and most energetic PeV event (ID 35) is at present without likely counterparts. NGC 253 (ID 10), which is the only starburst galaxy in our sample, is too weak when compared to other candidates. Same story for Centaurus A (ID 35), which is the only radio galaxy in our sample and an all-time favoured as a potential source by the cosmic ray community.

For completeness, we have also checked that our neutrino fluxes are consistent with the IceCube upper limits provided by Aartsen et al. (2013) (see their Tab. 2 and 3) assuming an  $E^{-2}$  ( $\nu^{-1}$ ) spectrum. This is especially important for the northern sources, where the neutrino non-detections are particularly stringent and at the level of the fluxes here derived (within the rather larger error bars). If the proposed counterparts in Tab. 4 are indeed neutrino sources, this suggests that a direct detection by IceCube is within reach.

To check the significance of our cross-correlations, we have re-done them by shifting the positions of the  $\gamma$ -ray catalogues by varying amounts always larger than the largest error radius ( $\geq 20^\circ$ ). Based on this, the chance of having seven or more neutrino events associated with TeVCat sources is  $\sim 64\%$ , which reduces to  $\sim 50\%$  for five neutrino events and blazar only counterparts. This simply reflects the incompleteness of TeVCat<sup>10</sup>. As regards WHSP, the chance of having eight neutrino events associated with that sample is 4%, while that of having 16 neutrino events associated with 1FHL sources is  $\sim 4\%$ , with the same probability for

1FHL blazars only becoming  $\sim 2\%$ . Even if some of these values are intriguing, we are fully aware that, having used the median angular errors for the neutrino events as given by the IceCube team provides only lower limits to these numbers.

We stress that, while better statistics are undoubtedly needed on the neutrino side, we have also shown that more TeV observations reaching also higher energies than currently available are badly needed to bridge the gap between photon and neutrino energies. Moreover, based on the energies and fluxes listed in Tab. 1, the merging of “classical” and neutrino astronomy will require sensitivities  $\approx 4 \times 10^{-11}$  erg cm<sup>-2</sup> s<sup>-1</sup> at  $E \approx 140$  TeV and  $\approx 3 \times 10^{-11}$  erg cm<sup>-2</sup> s<sup>-1</sup> at  $E \approx 1$  PeV. We note that, while the former values are within reach of the Cherenkov Telescope Array (CTA) even for relatively short exposure times (see Fig. 7 of Barnacka et al. 2013), the latter are not, as the maximum energy that CTA is expected to reach is only  $\sim 100$  TeV. Needless to say, all high FoM WHSP sources, but in particular those in Tab. 2, are obvious targets for current TeV facilities.

Further upcoming IceCube observations will be able to confirm or disprove the associations suggested here. We can think of two possible future scenarios:

- if our conclusions are proven to be wrong, this will mean the following: 1. the existence of a (new?) population of *Fermi*(1FHL)-undetected TeV sources either still to be detected, given the poor sky coverage of TeV telescopes, or totally absorbed by the extragalactic background light; in the latter case, the high-energy neutrino background will not be resolved into individual sources and will remain *diffuse* (in IceCube lingo); 2. a complete decoupling between  $\gamma$ -ray photons and neutrino production in the Universe; 3. a mixture of the two scenarios described above. In all these cases, the identification of neutrino sources will be extremely challenging;

- if our conclusions are at least partially confirmed, we will have shown for the first time the unambiguous presence of hadronic processes in blazars and pulsar wind nebulae, with very important consequences for our understanding of jet and high-energy astrophysics.

<sup>10</sup> As shown by taking a random half of the WHSP sample and obtaining a value of  $\sim 55\%$  for four neutrino events, which is much larger than the probability derived for the whole sample, as detailed here.

## 5 CONCLUSIONS

We have taken a very simple approach to tackle the issue of the astronomical counterparts of the IceCube neutrinos by looking for high-energy ( $\gtrsim 10$  GeV) sources within the error circles of the events. We found counterparts for sixteen out of the eighteen events considered in this work. By studying their hybrid photon – neutrino SEDs we have narrowed down our search and come up with a list of most probable counterparts for nine IceCube neutrinos. Interestingly, there is no single class of sources, which we can connect the IceCube events with. Instead, the available data suggest a mixed scenario of Galactic and extra-galactic neutrino sources. These include BL Lacs of the HSP type (i.e. with peak of the synchrotron emission at  $\nu > 10^{15}$  Hz) and pulsar wind nebulae. The still TeV-undetected sources, which we have singled out as probable neutrino counterparts, are obvious candidates for detection by current TeV facilities. CTA should reach the sensitivities required for a merging of “classical” and neutrino astronomy at  $\approx 100$  TeV. Further upcoming IceCube observations will be able to confirm or disprove the associations suggested here. Whatever the outcome of these tests, this will have crucial implications for blazar jets, high-energy astrophysics, and cosmic-ray and neutrino astronomy.

## ACKNOWLEDGMENTS

We thank Paolo Giommi, Stefan Coenders, Luigi Costamante, Andreas Gross, and Sirin Odrowski for useful discussions and suggestions and the many teams, which have produced the data and catalogues used in this paper for making this work possible. E. R. is supported by a Heisenberg Professorship of the Deutsche Forschungsgemeinschaft (DFG RE 2262/4-1). We acknowledge the use of data and software facilities from the ASDC, managed by the Italian Space Agency (ASI). This research has made use of the VizieR catalogue access tool, CDS, Strasbourg, France and of the NASA/IPAC Extragalactic Database (NED), which is operated by the Jet Propulsion Laboratory, California Institute of Technology, under contract with the National Aeronautics and Space Administration.

## REFERENCES

Aartsen M. G., et al., 2013, *PhRvL*, 111, 021103  
Aartsen M. G., et al., 2013, *ApJ*, 779, 132  
Abbasi R., et al., 2012, *Nature*, 484, 351  
Abdo A. A., et al., 2010, *ApJ*, 716, 30  
Abramowski A., et al., 2012, *ApJ*, 757, 158  
Acero F., et al., 2013, *ApJ*, 773, 77  
Ackermann M., et al., 2012, *ApJ*, 753, 83  
Ackermann M., et al., 2013, *ApJS*, 209, 34  
Aharonian F., et al., 2002, *A&A*, 393, 89  
Aharonian F., 2004, *Very high energy cosmic gamma radiation: a crucial window on the extreme Universe* (River Edge, NJ: World Scientific Publishing)  
Aharonian F., et al., 2004, *A&A*, 425, L13  
Aharonian F., et al., 2006, *A&A*, 456, 245  
Aharonian F., et al., 2008, *A&A*, 477, 353  
Aleksić J., et al., 2012, *ApJ*, 748, 46

Arsioli B., Fraga B., Giommi P., Padovani P., Marrese M., 2014, *A&A*, submitted  
Asano K., Mészáros P., 2014, *ApJ*, 785, 54  
Barnacka A., Bogacz L., Grudzińska M., Frankowski A., Janiak M., Lubiński P., Moderski R., for the CTA Consortium, 2013, *Proceedings ICRC2013, Rio de Janeiro (Brazil)* (arXiv:1307.3409)  
Bednarek W., 2003, *A&A*, 407, 1  
Böttcher M., Reimer A., Sweeney K., Prakash A., 2013, *ApJ*, 768, 54  
Carrigan S., Brun F., Chaves R. C. G., Deil C., Gast H., Marandon V., for the H. E. S. S. collaboration, 2013, *Proceedings of the 48th Rencontres de Moriond (2013), La Thuile (Italy)* (arXiv:1307.4868)  
Costamante L., 2012, 2011 Fermi Symposium proceedings, arXiv:1208.0808  
Dermer C. D., Atoyan A., 2001, *Proc. 27th ICRC, Hamburg, Germany* (arXiv:astro-ph/0107200)  
Fang K., Fujii T., Linden T., Olinto A. V., 2014, *ApJ*, submitted (arXiv:1404.6237)  
Fox D. B., Kashiyama K., Mészáros P., 2013, *ApJ*, 774, 74  
Franceschini A., Rodighiero G., Vaccari M., 2008, *A&A*, 487, 837  
Gehrels N., 1986, *ApJ*, 303, 336  
Giacinti G., Kachelriess M., Semikoz D. V., 2014, *ApJ*, submitted (arXiv:1403.3380)  
Giommi P., et al., 2012, *A&A*, 541, A160  
Giommi P., Padovani P., Polenta G., Turriziani S., D’Elia V., Piranomonte S., 2012, *MNRAS*, 420, 2899  
Giommi P., Padovani P., Polenta G., 2013, *MNRAS*, 431, 1914  
Halzen F., Vazquez R. A., 1993, *ICRC*, 1, 447  
HESS Collaboration, et al., 2013, *MNRAS*, 434, 1889  
Holder J., 2012, *APh*, 39, 61  
IceCube Collaboration, 2013, *Sci*, 342, 1242856  
IceCube Collaboration, 2014, *Physical Review Letters*, submitted (arXiv:1405.5303)  
Kampert K.-H., for the Pierre Auger Collaboration, 2012, *Proceedings ICRC 2011, Beijing, China* (arXiv:1207.4823)  
Kelner S. R., Aharonian F. A., Bugayov V. V., 2006, *PhRvD*, 74, 034018  
Kelner S. R., Aharonian F. A., 2008, *PhRvD*, 78, 034013  
Mannheim K., 1999, *APh*, 11, 49  
Massaro F., D’Abrusco R., Paggi A., Masetti N., Giroletti M., Tosti G., Smith H. A., Funk S., 2013, *ApJS*, 209, 10  
Murase K., Inoue Y., Dermer C. D., 2014, *arXiv*, arXiv:1403.4089  
Nolan P. L., et al., 2012, *ApJS*, 199, 31  
Padovani P., Giommi P., 1995, *ApJ*, 444, 567  
Padovani P., Giommi P., Rau A., 2012, *MNRAS*, 422, L48  
Protheroe R. J., 1997, *ASPC*, 121, 585  
Renaud M., Hoppe S., Komin N., Moulin E., Marandon V., Clapson A.-C., 2008, *AIPC*, 1085, 285  
Saba I., Tjus J. B., Halzen F., 2013, *APh*, 48, 30  
Schönert S., Gaisser T. K., Resconi E., Schulz O., 2009, *PhRvD*, 79, 043009  
Şentürk G. D., Errando M., Böttcher M., Mukherjee R., 2013, *ApJ*, 764, 119  
Tamborra I., Ando S., Murase K., 2014, *JCAP*, submitted (arXiv:1404.1189)

- Taylor A. M., Gabici S., Aharonian F., 2014, *PhRvD*, 89, 103003
- Urry C. M., Padovani P., 1995, *PASP*, 107, 803
- Villante F. L., Vissani F., 2008, *PhRvD*, 78, 103007
- Yoaast-Hull T. M., Gallagher J. S., III, Zweibel E. G., Everett J. E., 2014, *ApJ*, 780, 137